

Identification of an Intestinal Folate Transporter and the Molecular Basis for Hereditary Folate Malabsorption

Andong Qiu,^{1,2} Michaela Jansen,³ Antoinette Sakaris,⁴ Sang Hee Min,¹ Shrikanta Chattopadhyay,¹ Eugenia Tsai,^{1,2} Claudio Sandoval,⁵ Rongbao Zhao,^{1,2} Myles H. Akabas,^{1,3} and I. David Goldman^{1,2,*}

¹Department of Medicine

²Department of Molecular Pharmacology

³Department of Physiology and Biophysics

⁴Department of Obstetrics and Gynecology

Albert Einstein College of Medicine, 1300 Morris Park Avenue, Bronx, NY 10461, USA

⁵Department of Pediatrics, New York Medical College, Valhalla, NY 10595, USA

*Contact: igoldman@aecom.yu.edu

DOI 10.1016/j.cell.2006.09.041

SUMMARY

Folates are essential nutrients that are required for one-carbon biosynthetic and epigenetic processes. While folates are absorbed in the acidic milieu of the upper small intestine, the underlying absorption mechanism has not been defined. We now report the identification of a human proton-coupled, high-affinity folate transporter that recapitulates properties of folate transport and absorption in intestine and in various cell types at low pH. We demonstrate that a loss-of-function mutation in this gene is the molecular basis for hereditary folate malabsorption in a family with this disease. This transporter was previously reported to be a lower-affinity, pH-independent heme carrier protein, HCP1. However, the current study establishes that a major function of this gene product is proton-coupled folate transport required for folate homeostasis in man, and we have thus amended the name to PCFT/HCP1.

INTRODUCTION

Folates are essential cofactors that are required for the provision of one-carbon moieties in key biosynthetic and epigenetic processes (Stover, 2004). Folate deficiency is prevalent in underdeveloped countries, and even in the Western world, subtle deficiency is a public health problem that is most notable in its association with neural tube defects in the developing embryo (Eichholzer et al., 2006). Mammals cannot synthesize folates; hence, dietary sources must meet metabolic needs, necessitating an efficient intestinal absorptive mechanism. Absorption of folates occurs primarily in the duodenum and upper jejunum

and involves a carrier-mediated process with a low-pH optimum that operates efficiently within the acidic microclimate of the intestinal surface in this region (Selhub and Rosenberg, 1981; Mason and Rosenberg, 1994; McEwan et al., 1990). The specificity and other properties of this process have been well established, and similar folate transport activities with a low-pH optimum have been identified in other normal tissues and in human solid tumor cell lines (Horne, 1993; Zhao et al., 2004). Despite the prevalence and importance of this process, a folate transport protein with a low-pH optimum has not been identified.

There are two known highly specific mammalian folate transporters. Their properties were the subject of a recent review (Matherly and Goldman, 2003). The reduced folate carrier (SLC19A1) is a facilitative transporter with the characteristics of an anion exchanger. There are two GPI-linked folate receptors, high-affinity binding proteins that mediate cellular uptake by an endocytic mechanism. Folate receptor expression in small intestine is negligible. While the reduced folate carrier is expressed on the brush border membrane of intestinal cells, this transporter has a neutral pH optimum and a specificity profile that differs substantially from that observed in intestinal folate absorption and transport into intestinal cells and cells of other tissue origin at low pH (Selhub and Rosenberg, 1981; Mason and Rosenberg, 1994; Wang et al., 2004). Further, when reduced folate carrier function is lost due to deletion, mutation, or loss of expression of the gene, the low-pH folate transport activity remains intact (Zhao et al., 2004, 2005b; Wang et al., 2005).

This report describes the identification of a proton-coupled, electrogenic, high-affinity folate transporter with properties that are similar to folate transport in intestinal and other cells at low pH. A database mining approach was utilized based on the conserved amino acid sequence of SLC19 family members and the screening of candidate mRNAs in cell lines developed in this laboratory in which the reduced folate carrier was deleted but the

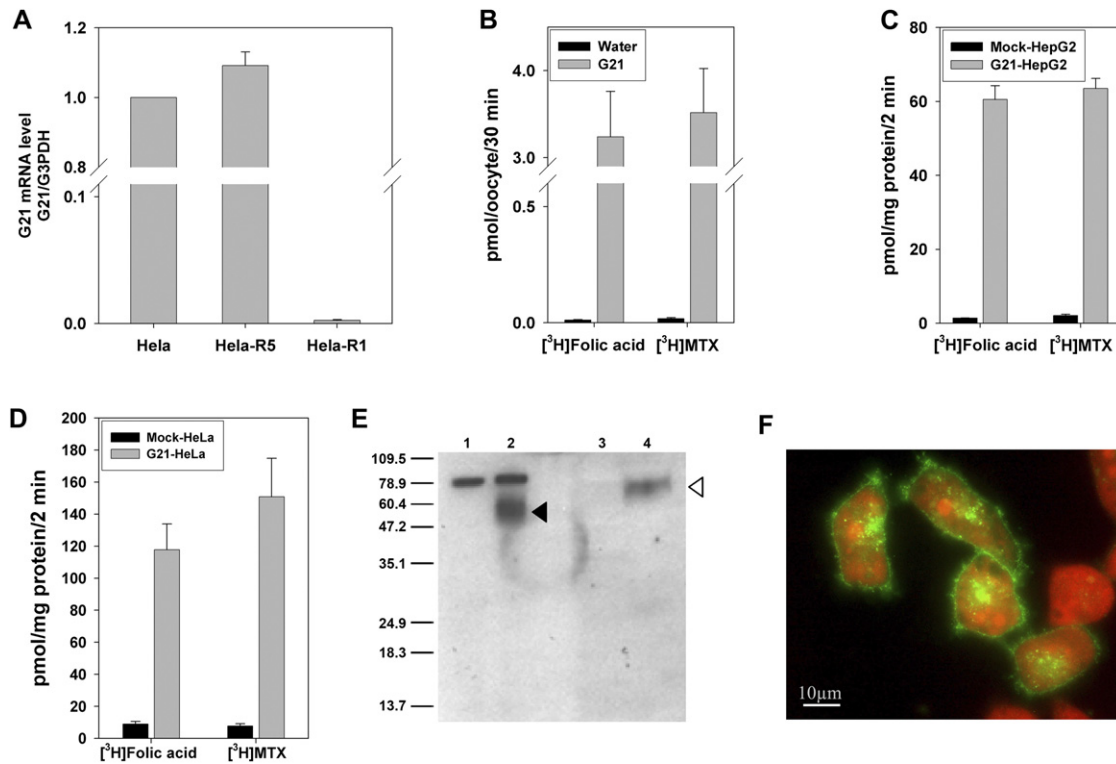


Figure 1. Identification and Initial Characterization of the Low-pH Folate Transporter

(A) G21 mRNA levels in HeLa, HeLa-R5, and HeLa-R1 cells determined by quantitative RT-PCR; G21 mRNA in HeLa cells was assigned the value of 1. The values are the mean \pm SEM for two independent experiments. (B) Functional expression of G21 in *Xenopus* oocytes. [³H]MTX or [³H]folic acid (2 μ M) uptake was assayed at pH 5.5 over 30 min. (C) Initial uptake of [³H]MTX or [³H]folic acid (0.5 μ M), at pH 5.5 and 37°C, into HepG2 cells stably transfected with pcDNA3.1(+) (Mock-HepG2) or pcDNA3.1(+)-G21 (G21-HepG2). (D) Initial uptake of [³H]MTX or [³H]folic acid (0.5 μ M), at pH 5.5 and 37°C, into HeLa cells transiently transfected with pcDNA3.1(+) (Mock-HeLa) or pcDNA3.1(+)-G21 (G21-HeLa). The data in (B)–(D) are the mean \pm SEM from three independent experiments. (E) Detection of G21 protein expressed in *Xenopus* oocytes and HepG2 cells by SDS-PAGE and western blotting. Lane 1: water-injected oocytes; lane 2: G21-cRNA injected oocytes; lane 3: mock-transfected HepG2 cells; lane 4: G21-transfected HepG2 cells. The blot is representative of three independent experiments. (F) Plasma membrane localization of G21 protein in HeLa cells transiently transfected with G21 cDNA detected by immunofluorescence. The green fluorescence shows the localization of G21 protein, and the red fluorescence indicates the counterstaining by propidium iodide. The image shown is representative of three independent studies.

low pH activity was either retained or markedly decreased (Zhao et al., 2004, 2005a). Having identified this carrier as a candidate intestinal folate transporter, we demonstrate a loss-of-function mutation in this gene in a family with the syndrome of hereditary folate malabsorption.

RESULTS

Identification of a Low-pH Folate Transporter

To identify the low-pH folate transporter, the Ensembl human peptide database was mined at low stringency as described in the [Experimental Procedures](#). Twenty-three human genes encoding membrane proteins with unknown functions were identified, and mRNA expression levels were screened in two HeLa cell lines developed in this laboratory: (1) the HeLa-R5 (Zhao et al., 2004) cell line, which has a genomic deletion of the reduced folate carrier gene but a high level of low-pH folate transport activity and (2) the HeLa-R1 line (Zhao et al., 2005a), a HeLa-R5 derivative, cloned by antifolate selective pressure, in which the

low-pH activity is markedly diminished. Gene 21 (to be referred to as G21) was identified in this screen as a likely candidate based on a high mRNA level in HeLa-R5 cells versus a very low level of expression in HeLa-R1 cells (Figure 1A). G21 (GenBank accession number NP_542400) is predicted to be a membrane protein of 459 amino acids with a MW of \approx 50 kDa. A BLAST search of the Swissprot database revealed that the human protein shares 91% similarity and 87% identity to both its mouse and rat counterparts (GenBank accession numbers AAH57976 and AAH89868). During the course of the studies described below, this protein was reported by another group to be a heme carrier protein (HCP1) and entered into GenBank as such (Shayeghi et al., 2005). This protein was designated as SLC46A1 in the Human Genome Organization (HUGO) Nomenclature Committee Database.

Folate transport properties mediated by this carrier were assessed by injection of G21 cRNA into *Xenopus laevis* oocytes. As indicated in Figure 1B, uptake of 2 μ M [³H]folic acid and [³H]methotrexate (MTX) was increased

>200-fold in G21 cRNA-injected oocytes at pH 5.5 as compared to water-injected oocytes. Similarly, uptake of these folates into HepG2 cells stably transfected with G21 cDNA (Figure 1C) and into HeLa cells transiently transfected with G21 cDNA (Figure 1D) was increased >30- and >13-fold, respectively. A western blot using a polyclonal antibody directed to the C terminus of G21 indicated a broad band in G21 cRNA-injected, but not water-injected, *Xenopus* oocytes and in HepG2 cells stably transfected with this cDNA, but not in mock-transfected cells (Figure 1E). Differences in migration in the two systems may be due to differences in glycosylation. When expressed in HeLa cells, G21 protein targeted to the plasma membrane in permeabilized cells as demonstrated with the polyclonal antibody (Figure 1F). Staining could not be detected in mock-transfected HeLa cells (data not shown).

The pH Dependence of G21-Mediated Transport

Transport of folates mediated by G21 was highly pH dependent, as illustrated for tritiated folic acid (Figure 2A), (6S)5-methyltetrahydrofolate [(6S)5-MTHF, Figure 2B], MTX (Figure S1A in the Supplemental Data available with this article online), and (6S)5-formyltetrahydrofolate [(6S)5-FTHF; Figure S1B]. Activity was highest at the lowest pH and declined as the pH was increased, although the pattern of decrease, and the extent of retention of activity at neutral pH, was different among the folates. For both (6S)5-MTHF, the major blood folate in man and rodents, and (6S)5-FTHF, there was residual activity at pH 7.5, and for all the folates there was substantial activity at pH 6.5. The dependence of G21 activity on the inward-directed electrochemical H^+ gradient was further characterized by exposure of *Xenopus* oocytes to carbonyl cyanide 4-(trifluoromethoxy) phenylhydrazone (FCCP), an ionophore that collapses the transmembrane H^+ gradient (Benz and McLaughlin, 1983). As shown in Figure 2C and Figure S1C, respectively, at an extracellular pH of 5.5, [3H]folic acid and [3H]MTX uptake were markedly decreased by 10 μM FCCP.

The Kinetics of Folate Transport Mediated by G21 as a Function of pH

Uptake mediated by G21 conformed to Michaelis-Menten kinetics with a K_m for [3H]folic acid uptake, which increased as pH increased, from $1.3 \pm 0.1 \mu M$ at pH 5.5 to $56.2 \pm 5.6 \mu M$ at pH 7.5 (Figures 2D–2H). V_{max} and K_m were evaluated as a function of pH using the same batch of oocytes, each injected with the same amount of G21 cRNA. As shown in Figure 2G, the V_{max} for folic acid uptake decreased from 13 pmol/oocyte/hr at pH 5.5 to 5 pmol/oocyte/hr at pH 7.5. The major change (2.4-fold) occurred over the pH range of 5.5 to 6.5, with only a small decline beyond pH 6.5. The pattern of change was different for the folic acid K_m measured at the same time. There was a small (2.6-fold) increase in K_m as the pH was increased from 5.5 to 7.0, but there was a 18-fold increase when the pH was increased from 7.0 to 7.5. Figure 2H

indicates a 2- to 3-fold higher uptake K_m for MTX as compared to folic acid over this pH range, with a similar pattern of increase as the pH was increased.

Structural Specificity of G21-Mediated Transport

Figure 3A shows the inhibitory effects of a variety of compounds, at a concentration of 20 μM , on uptake of 2 μM [3H]folic acid into *Xenopus* oocytes injected with G21 cRNA. There was a high degree of structural specificity among the folate/antifolate compounds tested; pemetrexed was the most potent competitor. This is an antifolate inhibitor of thymidylate synthase with the highest affinity for the low-pH transporter in human tumor cell lines (Zhao et al., 2005b; Wang et al., 2004). Transport is stereospecific; the natural 6S isomer of 5-FTHF was more potent than the unnatural 6R isomer in reducing [3H]folic acid uptake. The 6S isomer of 5-MTHF had effects comparable to those of (6S)5-FTHF. MTX was a less effective competitor than folic acid, consistent with the difference in transport K_m s. PT523 is a dihydrofolate reductase inhibitor with a high affinity for the reduced folate carrier at high and low pH but a very low affinity ($K_i > 50 \mu M$) for the low-pH folate transporter in HeLa and other cells (Zhao et al., 2005b; Wang et al., 2004). This antifolate did not inhibit under these conditions. All the folates that inhibited [3H]folic acid uptake are transport substrates of G21. Thus, the inhibition of [3H]folic acid uptake was due to competition for transport via G21. Figure 3B compares the structures of these folate compounds. The major difference between PT523 and the other folates/antifolates is at the γ -carboxyl moiety, suggesting the importance of this group to folate binding to G21. Bromosulphophthalein, para-aminohippuric acid, taurocholic acid, cholic acid, and estrone-3-sulfate, substrates for organic anion solute carriers (SLC21 and SLC 22) (Hagenbuch and Meier, 2003; Koepsell and Endou, 2004), did not inhibit [3H]folic acid influx. Hemin was a weak inhibitor. At a [3H]folic acid concentration of 2 μM , 100 μM hemin inhibited uptake by $42\% \pm 7\%$ in *Xenopus* oocytes injected with G21 cRNA and by $30\% \pm 5\%$ in HepG2 cells stably transfected with G21 cDNA. In the same experiments, 100 μM nonlabeled folic acid inhibited 2 μM [3H]folic acid uptake by $92\% \pm 2\%$ and $90\% \pm 0.02\%$, respectively (based on the average of three separate experiments at pH 6.5).

Electrophysiological Properties of G21-Mediated Transport in *Xenopus* Oocytes

Electrophysiological characteristics were evaluated in two-electrode voltage-clamp experiments. In G21 cRNA-injected oocytes, folic acid, (6S)5-MTHF, and MTX induced currents of up to 80 nA at a -80 mV holding potential (Figure 4A). These folates did not induce current in water-injected oocytes. These substrate-induced currents imply that net charge translocation occurred across the cell membrane during each transport cycle. Consistent with this, substrate currents were proportional to both applied voltage and substrate concentration, increasing

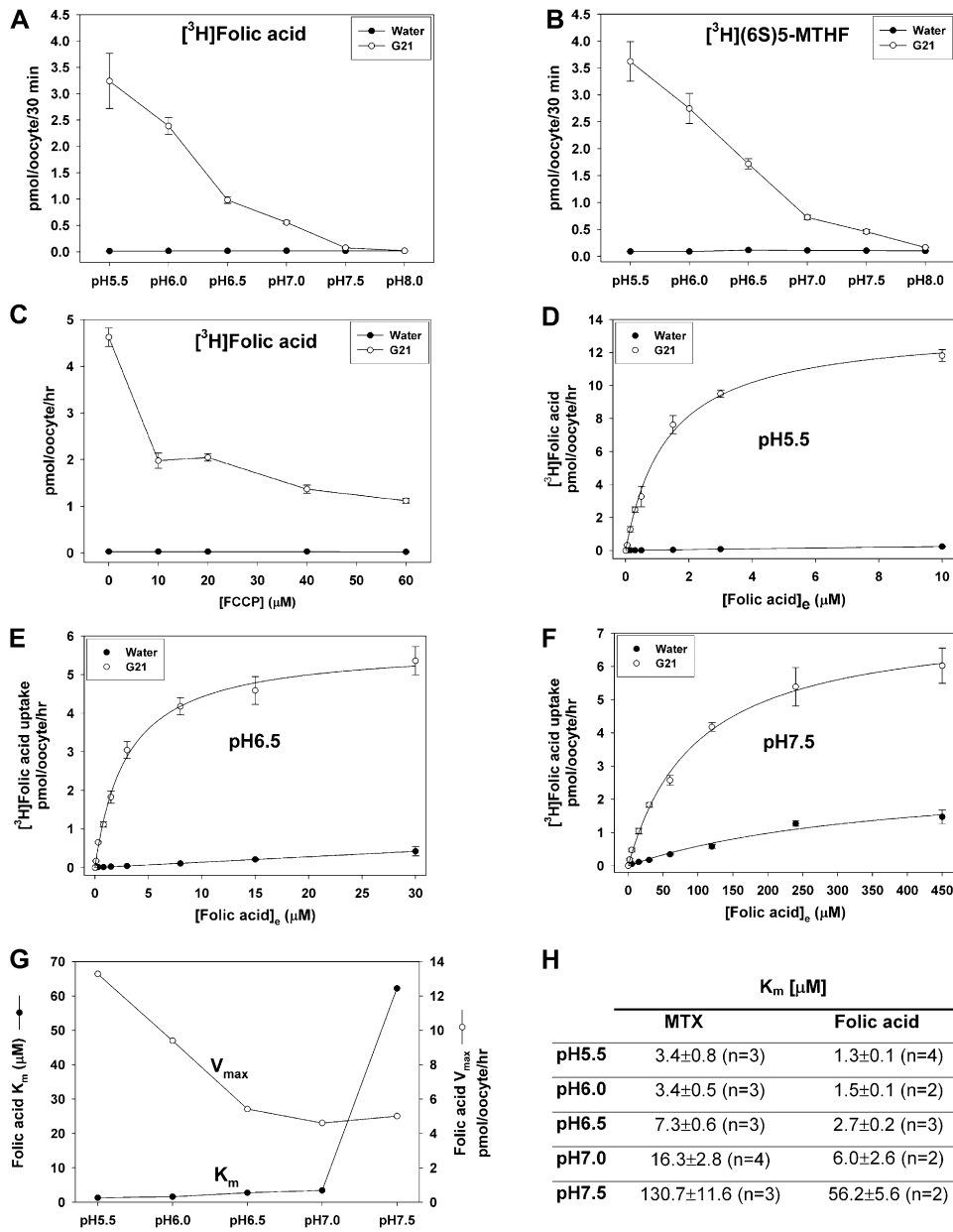


Figure 2. pH Dependence and Kinetics of G21-Mediated Uptake of Tritiated Folates in *Xenopus* Oocytes

(A and B) Uptake of 2 μM $[^3\text{H}]$ folic acid (A) and $[^3\text{H}](6\text{S})5\text{-MTHF}$ (B) in water- and G21 cRNA-injected oocytes over 30 min. (C) Water- and G21 cRNA-injected oocytes were preincubated at pH 5.5 with a series of FCCP concentrations for 20 min. Uptake of $[^3\text{H}]$ folic acid (2 μM) was subsequently assessed at pH 5.5 over 1 hr. (A)–(C) are representative of three independent studies. (D–F) Uptake of $[^3\text{H}]$ folic acid over 60 min at pH 5.5 (D), 6.5 (E), and 7.5 (F) as a function of the extracellular folic acid concentration, [Folic acid]_e. The lines were generated, and kinetic constants were calculated, based on Michaelis-Menten kinetics ($V = V_{max}[S]/(K_m + [S])$). The data are representative of two to four experiments as summarized in (H). (G) Effects of extracellular pH on $[^3\text{H}]$ folic acid uptake K_m and V_{max} . All measurements were made in a single batch of oocytes with the injection of the same amount of G21 cRNA. (H) A summary of uptake K_m for MTX and folic acid as a function of extracellular pH. All data are the mean \pm SEM.

with more negative voltage and higher substrate concentration (Figures 4B–4D and Figure 5).

In order to distinguish between whether folate transport was coupled to proton transport (i.e., protons are transported with the folate) or whether protons just bind to the transporter and regulate its activity, we determined

the effect of changing extracellular pH from 5.5 to 7.5 on the substrate current-voltage relationship. The reversal potential of the current-voltage relationship is the voltage at which the substrate-induced current is zero (the x axis intercept in Figures 4C and 4D) and is a measure of the net driving force for substrate transport. If folate and

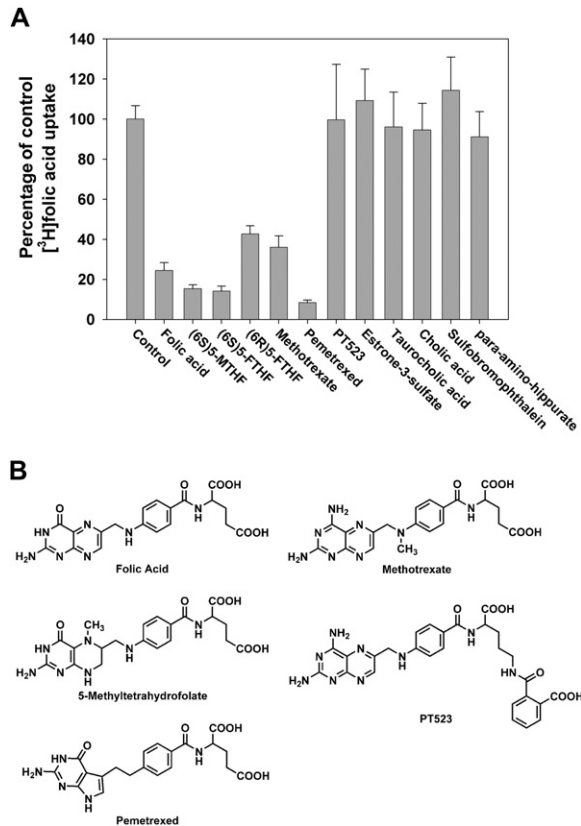


Figure 3. Substrate Specificity of G21 in *Xenopus* Oocytes
 (A) Uptake of 2 μM [^3H]folic acid was assessed at pH 5.5 over 30 min in the absence (control) or presence of 20 μM nonlabeled folates, antifolates, or other organic anions. The data are the mean \pm SEM of two independent experiments.
 (B) The structures of folate and antifolate compounds studied.

proton transport are coupled, then the reversal potential would become more negative as the extracellular pH is raised, and the slope would decrease. In contrast, if the folate transport rate were only regulated by pH, then the slope of the current-voltage relationship would decrease, but the reversal potential would not change. As the pH increased, the reversal potential became more negative (Figures 4C and 4D). Changing the pH from 5.5 to 6.5 shifted the reversal potentials for MTX and (6S)5-MTHF by -8 mV and -6 mV, respectively, whereas increasing the pH from 6.5 to 7.5 shifted the reversal potentials by -36 mV and -30 mV, respectively. This change in the reversal potential with a change in pH provides direct evidence that the transmembrane proton gradient is coupled to folate transport. These results are consistent with the loss of net proton influx driving transport, as the extracellular pH increased to a value comparable to an intracellular pH of ~ 7.3 . At pH 7.5, the transmembrane proton gradient is close to zero, and folate influx is driven solely by the folate concentration gradient due to the higher extracellular folate concentration. Thus, the reversal potential is more negative at pH 7.5 than at lower pHs where the

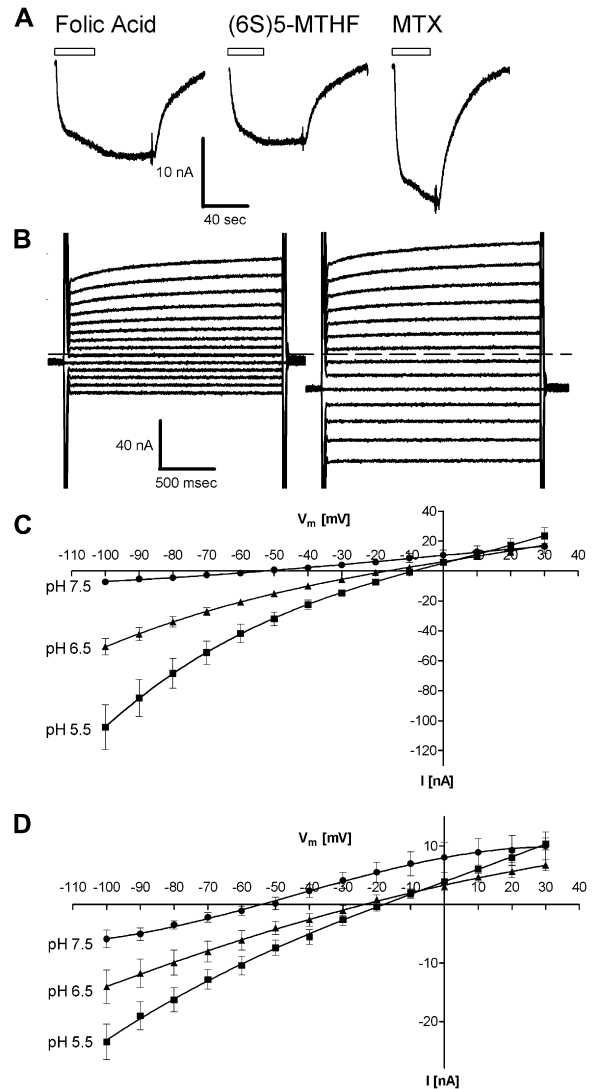


Figure 4. Electrophysiological Characterization of the G21 Transporter in *Xenopus* Oocytes

(A) Substrate-induced currents recorded by two-electrode voltage-clamp from G21 expressing oocytes at a -80 mV holding potential with concentrations of folates 20–25 times the K_m s at pH 5.5. Currents for all substrates were measured in individual oocytes ($n = 8$ oocytes). A representative experiment from one oocyte is shown.
 (B) Currents from a G21-expressing oocyte, left superfused with buffer at pH 5.5, right superfused with MTX at 25 times the K_m at pH 5.5. Responses to depolarizing and hyperpolarizing voltage-clamp steps are shown. Oocytes were held at -60 mV, and the voltage was stepped for 2 s in 10 mV increments from -100 mV to $+30$ mV. The dashed line indicates the level of $I = 0$.
 (C and D) Current-voltage relationships as a function of extracellular pH for MTX (C) and (6S)5-MTHF (D) with concentrations of 20–25 times the K_m s. Data are the mean \pm SEM for three to eight oocytes from two toads.

transmembrane proton gradient also contributes to the net driving force for transport.

Figure 5A shows the currents recorded from an individual oocyte as the extracellular MTX concentration was

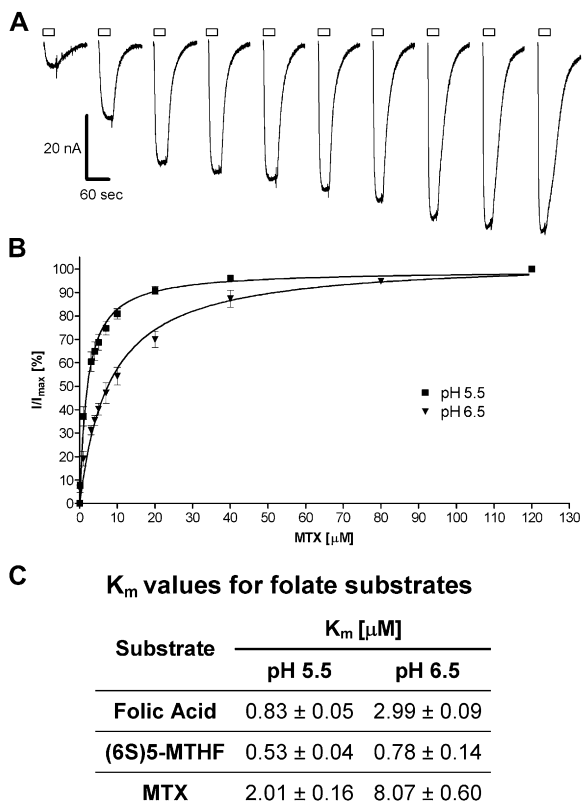


Figure 5. Concentration Dependence of Substrate-Induced Currents

(A) Currents recorded from an individual oocyte in response to (from left to right) 0.1, 1, 3, 4, 5, 7, 10, 20, 40, and 120 μM MTX (pH 5.5, $V_h = -80$ mV). Bars above current traces denote time of substrate application.

(B) Currents obtained as described in (A) at pH 5.5, and in similar experiments at pH 6.5, were normalized to the maximum current I_{max} for each oocyte and plotted as a function of substrate concentration. The normalized currents from different experiments were fit to the equation $I = (I_{\text{max}} \times [S]) / (K_m + [S])$ to obtain K_m . Data are the mean \pm SEM for three to eight oocytes from two toads.

(C) Summary of the electrophysiologically determined K_m values for folic acid, (6S)5-MTHF, and MTX as a function of extracellular pH. The data are the mean \pm SEM for three to seven experiments.

increased from 0.1 to 120 μM . Current was detected at a MTX concentration as low as 0.1 μM . Figure 5B illustrates the dependence of current on the MTX concentration at pH 5.5 and 6.5. The K_m s for folic acid, (6S)5-MTHF, and MTX (Figure 5C), and their pH dependence, were comparable in the electrophysiological and the tritiated substrate uptake assays (Figures 2H and 5C). The K_m s at pH 6.5 for folic acid and MTX were nearly four times greater than those at pH 5.5, while the K_m for (6S)5-MTHF was only minimally increased. The relative current magnitude induced by the different substrates was assessed by applying saturating concentrations of each substrate to the same oocyte at pH 5.5 (Figure 4A). When normalized to the (6S)5-MTHF-induced current magnitude, the current

amplitudes were $39\% \pm 6\%$ and $86\% \pm 11\%$ ($n = 8$) larger for folic acid and MTX, respectively, despite the fact that the latter substrates had higher K_m s (Figure 5C). This implies that the transport V_{max} for these substrates was higher than that for (6S)5-MTHF.

An attempt was made to determine if hemin transport could be detected by current flow into oocytes injected with G21 cRNA. In two separate experiments using two different batches of oocytes, three to four oocytes for each condition, folic acid produced substantial currents, while no current could be detected with 100 μM hemin either when hemin was stabilized with 0.1% bovine serum albumin or with 200 μM arginine (data not shown). If hemin were transported by G21 in an electrogenic fashion similar to the folates, then the "expected" currents from this approximately EC_{50} hemin concentration (reported hemin K_m of 125 μM [Shayeghi et al., 2005]) would be well within the detection limits of this system.

Lack of Impact of Other Extracellular Ions on G21-Mediated Transport into Oocytes

Substitution of extracellular Na^+ with N-methyl-glucosamine did not decrease [^3H]MTX uptake into G21 cRNA-injected oocytes, excluding a sodium-dependent process. Similarly, folic acid-induced currents were unchanged when K^+ , Ca^{2+} , or Mg^{2+} was removed from the extracellular solution or when the extracellular Cl^- concentration was reduced from 95.6 mM to 5.6 mM by replacement of NaCl with Na-gluconate. Thus, folate transport was not dependent on extracellular Na^+ , K^+ , Ca^{2+} , Mg^{2+} , or Cl^- , implying that none of these ions are involved in the folate transport cycle (data not shown).

G21 Expression in Human Tissues and Tumor Cell Lines

G21 mRNA levels were examined in a variety of human tissues by northern blotting (Figure 6A). After hybridization followed by high stringency washes, two G21 mRNA forms were detected with molecular sizes of ≈ 2.7 kb and 2.1 kb. The latter, short form was dominant, with a molecular size consistent with G21 mRNA in the NCBI database (2.096 kb; GenBank accession number NM_080669). Substantial amounts of both G21 mRNA forms were detected in kidney, liver, placenta, small intestine, and spleen, and to a lesser extent, in colon and testis. There was very low expression in brain, lung, stomach, heart, and muscle. A smaller G21 transcript (~ 1 kb) was detected in brain, heart, and kidney, and an even smaller transcript was detected in liver (~ 0.5 kb). Quantitative RT-PCR was employed to further quantify G21 mRNA expression in intestine along with two human tumor cell lines (Figure 6B). Expression in Caco2 cells, a colon carcinoma cell line, was >7 -fold higher than that in HeLa cells. In intestine, the highest level of mRNA expression was in duodenum, with lesser expression in jejunum and lower levels in ileum, cecum, segments of the colon, and rectum. Consistent with the northern blot, there was a high level of expression in liver.

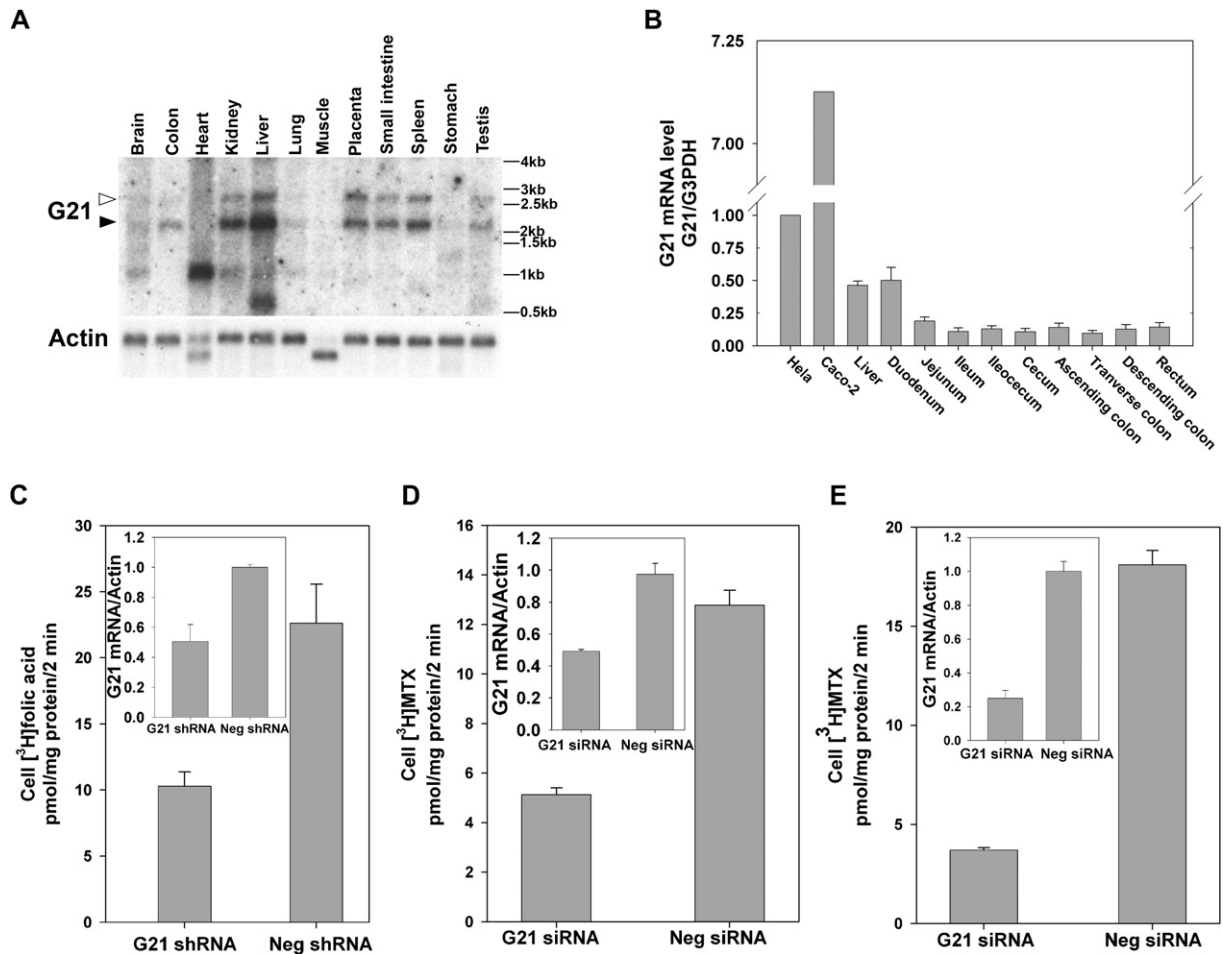


Figure 6. G21 mRNA Levels in Human Tissues and Tumor Cell Lines and Suppression of G21 Expression and Folate Transport Activity in Caco2 Cells by Interfering RNA

(A) Expression of G21 mRNA levels in human tissues by northern blotting. β -actin was the loading control. Open and filled triangles indicate the location of two G21 major mRNA transcripts. (B) G21 mRNA levels in two human cell lines and tissues were determined by quantitative RT-PCR. G3PDH mRNA was the house-keeping gene to normalize G21 expression. The ordinate represents expression of G21 mRNA relative to expression in HeLa cells assigned the value of 1. (C) The impact of stable transfection of G21 shRNA constructs into Caco2 cells on G21 mRNA levels determined by RT-PCR (inset) and uptake of [3 H]folic acid (0.5 μ M) at pH 5.5 and 37 $^{\circ}$ C for 2 min as compared to cells transfected with negative shRNA plasmids. (D) The impact of transient transfection of Caco2 cells with siRNA duplex, using the Amaxa system, on G21 mRNA (inset) and uptake of [3 H]MTX (0.5 μ M) at pH 5.5 and 37 $^{\circ}$ C for 2 min as compared to cells with scrambled (Neg) siRNA. (E) Caco2 cells stably transfected with the G21 shRNA constructs were subjected to transient transfection with siRNA duplex using the Amaxa system, and both G21 mRNA levels (inset) and uptake of [3 H]MTX (0.5 μ M) at pH 5.5 and 37 $^{\circ}$ C for 2 min were assessed. The data in (B)–(E) are the mean \pm SEM from three independent experiments.

The Impact of Suppression of G21 Expression by Interfering RNA on Folate Transport in Human Caco2 Cells

As indicated above, Caco2 cells have a very high level of G21 mRNA expression. To establish the extent to which constitutive low-pH folate transport activity in Caco2 cells could be attributed to this transporter, two small hairpin RNA (shRNA) vectors, targeted to two different regions of the G21 transcript, were stably cotransfected into Caco2 cells. This resulted in a 55% reduction in [3 H]folic acid influx at pH 5.5 and a similar (50%) decrease in G21 mRNA as quantified by RT-PCR (Figure 6C). Wild-type Caco2 cells

were subjected to transient transfection with small interfering RNA (siRNA) duplex using the Amaxa system, resulting in a 60% reduction in [3 H]MTX influx and a 50% decrease in G21 mRNA as compared to negative siRNA-transfected cells (Figure 6D). When the stably transfected Caco2 cells were also subjected to transient transfection with the Amaxa protocol, there was a further suppression of G21 mRNA, resulting in an 80% decrease in [3 H]MTX influx at pH 5.5 and a 75% decrease in G21 mRNA as compared to vector control-transfected cells (Figure 6E). Taken together, these studies demonstrate that G21 is the major, and possibly the only, low-pH folate transporter in Caco2 cells.

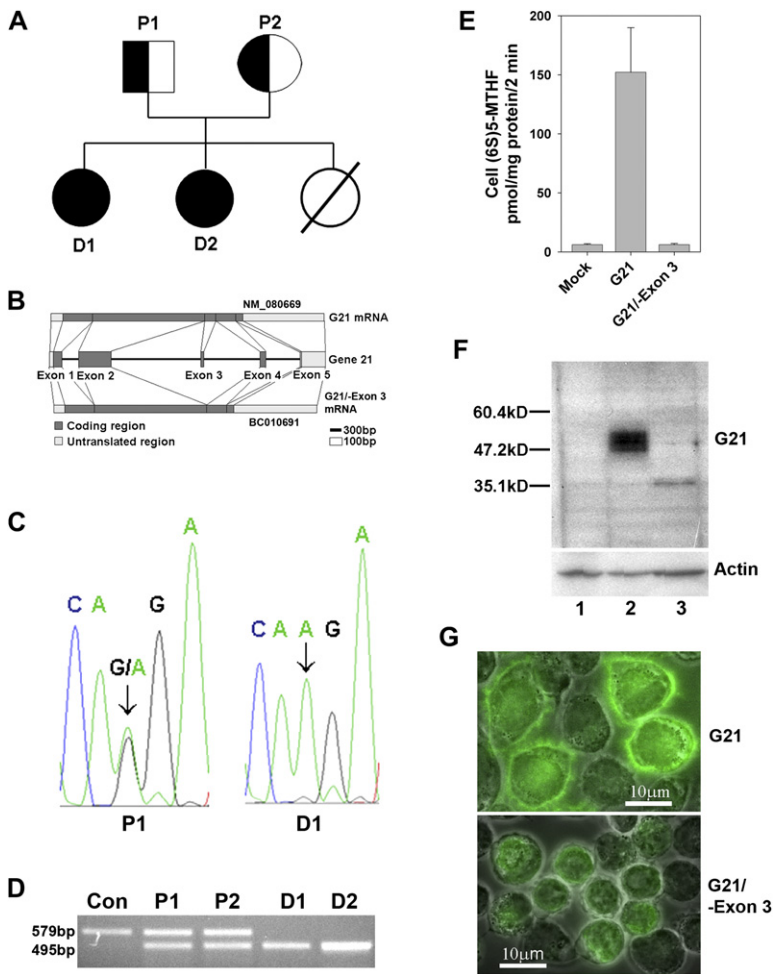


Figure 7. Genetic and Functional Analysis of G21 in a Family with Hereditary Folate Malabsorption Syndrome

(A) Pedigree of a family with hereditary folate malabsorption. P1 and P2 are the parents; D1 and D2 are the affected daughters. (B) Genomic organization of G21 and splicing of the wild-type and mutated G21 mRNA. (C) Representative chromatograms of sequenced DNA showing a heterozygous mutation in the father (P1) and a homozygous mutation in a daughter (D1) in G21. (D) Agarose gel analysis of RT-PCR products of mutated and wild-type G21 cDNA from family members. The control is a PCR fragment derived from normal human intestinal cDNA. (E) Functional analysis of exon 3-deleted G21 in HeLa cells. Exon 3-deleted (G21/-Exon 3), wild-type G21 cDNA (G21), and empty plasmid vector (Mock) were transiently transfected into HeLa cells. Uptake of (6S)[³H]5-MTHF (0.5 μM) was examined at pH 5.5 and 37°C over 2 min. The data are the mean ± SEM for four independent experiments. (F) Western blot analysis of wild-type (lane 2) and exon 3-deleted (lane 3) G21 proteins in transiently transfected HeLa cells. Empty plasmid (Mock) was transfected into HeLa cells as a control (lane 1). β-actin was the loading control. The blot is representative of three independent experiments. (G) Subcellular localization of wild-type (G21) and exon 3-deleted (G21/-Exon 3) G21 proteins expressed in transiently transfected HeLa cells as determined by immunofluorescence. The image shown is representative of three independent studies.

An Analysis of the Role of G21 in the Pathogenesis of Hereditary Folate Malabsorption in a Family with This Disease

Hereditary folate malabsorption (OMIM 229050) is a rare recessive familial disorder characterized by signs and symptoms of folate deficiency that appear within a few months after birth. Infants exhibit low blood and cerebrospinal fluid folate levels with anemia, diarrhea, immune deficiency, infections, and neurological deficits. There is a profound defect in intestinal folate absorption (Geller et al., 2002). To determine whether an alteration in G21 is the molecular basis for this disorder, blood was obtained from a family with progeny manifesting this disease that were the subject of a recent report (Geller et al., 2002; Figure 7A). The mother and father were both normal, one of their children died in infancy, and two of their other daughters displayed classical signs and symptoms of hereditary folate malabsorption. One daughter was diagnosed at the age of 8 months with a serum folate level of 0.2 nM (normal: 10–30 nM), and the other daughter was diagnosed at the age of 2 months with a blood folate level of less than 0.2 nM. Both children were treated with high doses of oral 5-FTHF with complete resolution of the signs

and symptoms of their disease; they have developed normally and remain completely well on their folate supplement now at ages 9 and 6.

G21 is composed of five exons and four introns (Figure 7B). Each of the five exons of G21 along with their flanking intron regions was sequenced from these family members. This revealed a homozygous mutation in G21 from both daughters and the same mutation in one allele of G21 from each parent (Figure 7C). This G to A mutation (position 5882; GenBank accession number DQ496103) is located in the splice acceptor of intron 2 (intron 2/exon 3 boundary). To determine the consequences of this genomic mutation on RNA splicing, the exon 3 region of G21 mRNA was analyzed by RT-PCR from these family members. Two DNA fragments of 579 bp and 495 bp were detected from the parents' transformed lymphocyte cDNAs, whereas in the daughters only a single DNA fragment was detected with a size identical to the shorter fragment from the parents. In comparison, the control cDNA from normal intestine exhibited a single amplified DNA fragment that was identical in size to the longer DNA fragment from the parents (Figure 7D). Subsequent DNA sequencing showed that the longer DNA fragment contained exon 3,

whereas the shorter one did not. Hence, the single-nucleotide mutation of G21 results in skipping of exon 3 and consequent in-frame deletion of 28 amino acids. Interestingly, the cDNA of this mutated transporter can be found in the GenBank (accession number BC010691) and appears to represent an alternatively spliced form (Figure 7B). When transiently transfected into HeLa cells, this mutated G21 carrier lacked transport function based on an analysis of (6S)5-MTHF uptake (Figure 7E). Western blot analysis showed that the mutated G21 protein was less efficiently expressed and had a lower molecular weight than the wild-type protein when transiently transfected into HeLa cells (Figure 7F). Further, immunofluorescence analysis indicated that, when expressed in HeLa cells, the mutated G21 carrier was trapped intracellularly without detectable localization to the cell membrane (Figure 7G). Thus, the parents carried both a functional wild-type and the non-functional mutated G21 mRNA, and the daughters with the disease had only the nonfunctional mutated G21 mRNA. No mutation was detected in the reduced folate carrier mRNA amplified from the transformed lymphocyte cDNA from both daughters.

DISCUSSION

These studies have identified G21, previously identified as HCP1 (SLC46A1), as a proton-coupled, electrogenic folate transporter that has the properties of the low-pH folate transport activity associated with transport of folates in intestinal and other human cells—a high affinity for folic acid ($K_i \sim 0.6 \mu\text{M}$) and a low affinity for the PT523 antifolate ($K_i \sim >50 \mu\text{M}$) at pH 5.5. This is in contrast to what is observed for the reduced folate carrier, a facilitative transporter (SLC19A1) ubiquitously expressed in human tissues. This carrier has low affinity for folic acid ($K_i \sim 200 \mu\text{M}$), high affinity for PT523 ($K_i \sim 0.7 \mu\text{M}$), and a pH optimum of 7.4. The affinity of the reduced folate carrier for these folates, also in contrast to the low-pH transporter, does not change appreciably between pH 5.5 and 7.4 (Matherly and Goldman, 2003; Wang et al., 2004).

The identification of a loss-of-function mutation in *hcp1* that results in the deletion of the third exon in a family with hereditary folate malabsorption establishes that this gene is an intestinal transporter required for normal folate absorption and homeostasis. Accordingly, we amend the name of the transporter to PCFT/HCP1. This takes into consideration the fact that this carrier is expressed in other tissues and may have functions beyond intestinal folate absorption. Consistent with the role of PCFT/HCP1 in intestinal absorption are the following observations: (1) PCFT/HCP1 mRNA is expressed in small intestine, particularly in the duodenum and to a lesser extent in jejunum, segments that account for the bulk of folate absorption. These are areas in which the pH at the microenvironment of the intestinal surface is in the range of 6.0–6.2 (McEwan et al., 1990). (2) PCFT/HCP1 protein is localized to the apical brush border of intestinal cells (Shayeghi et al., 2005). (3) PCFT/HCP1 is highly expressed in Caco2 cells, which

manifest a high level of low-pH folate transport activity and have been used as a model for intestinal transport (Hidalgo et al., 1989). (4) This constitutive folate transport activity in Caco2 cells can be nearly abolished (~80% suppression) by PCFT/HCP1 interfering RNA. The pH dependence of folate transport mediated by PCFT/HCP1 is consistent with studies in everted jejunal sacs and rings (Mason and Rosenberg, 1994). Quantitatively, in rat jejunum brush border membranes the uptake K_m for folic acid increased from $0.6 \mu\text{M}$ at pH 5.5 to $12.3 \mu\text{M}$ at pH 7.4 and was competitively inhibited ($K_i = 1.4 \mu\text{M}$) by racemic 5-MTHF (Mason et al., 1990; Selhub and Rosenberg, 1981). The identification of this carrier not only confirms the earlier conclusion that low-pH folate transport must be mediated by a mechanism genetically distinct from the reduced folate carrier, but also argues against an important role for the reduced folate carrier in intestinal folate absorption, as has been proposed (Said, 2004). Hence, while the reduced folate carrier is expressed in the upper small intestine, its activity must be negligible since it cannot compensate for the loss of the PCFT/HCP1 in individuals with hereditary folate malabsorption under the acidic conditions of the absorptive surface. Likewise, the level of reduced folate carrier expression and function in the more alkaline distal small intestinal compartments is, apparently, insufficient to meet folate requirements at usual dietary folate levels. However, with the pharmacologic doses of 5-FTHF that are used to treat individuals with this disease (Geller et al., 2002), this mechanism may be the route of delivery under these conditions.

This transporter was recently reported to be an intestinal heme carrier protein (HCP1). The murine ortholog was characterized as pH independent over a range of 6.5 to 8.0 and with a K_m of $125 \mu\text{M}$ for [^{55}Fe]hemin uptake in HeLa cells infected with a cDNA-containing adenovirus vector (Shayeghi et al., 2005). In that study, only a low level of transport activity was observed in *Xenopus* oocytes microinjected with the murine cRNA. Transporter mRNA was highly expressed in duodenum, and protein was localized to the apical brush border membrane of murine intestinal cells. We found that hemin was an inhibitor of folic acid uptake into both *Xenopus* oocytes injected with PCFT/HCP1 cRNA and HepG2 cells stably transfected with this carrier. However, we were unable to detect a hemin-induced current in *Xenopus* oocytes expressing this transporter under conditions in which currents for the folate compounds were easily detectable. This implies that either there is no electrogenic hemin transport or that the V_{max} for hemin transport must be more than an order of magnitude lower than that of folic acid. Based on the high affinity of this transporter for folates (approximately two orders of magnitude greater than the reported affinity for [^{55}Fe]hemin), the high degree of specificity (including stereospecificity) for the folate/antifolate compounds, and the etiologic role of the mutated protein as the molecular basis for hereditary folate malabsorption, it is clear that folates are major physiological substrates for this transporter. Further, the apparent complete correction of the hematological

disorder with high doses of folates in individuals with hereditary folate malabsorption who lack both wild-type copies of this gene argues against an important role of this carrier in the intestinal absorption of iron (Geller et al., 2002).

While PCFT/HCP1 operates most optimally at low pH, there is residual transport activity for 5-MTHF, the major blood folate (Opladen et al., 2006), at pH 7.4, suggesting that PCFT/HCP1 plays a role in the delivery of this folate to systemic cells under physiological conditions. Hence, the physiological importance of PCFT/HCP1 may extend to other organs in which PCFT/HCP1 mRNA is expressed, especially where transport activity at low pH has been documented, i.e., liver, which is a major folate storage site (Horne, 1993), but an acidic microenvironment is not present. From a pharmacological perspective, PCFT/HCP1 may play an important role in the delivery of antifolates into the acidic interior of solid tumors (Helmlinger et al., 1997; Wike-Hooley et al., 1984). The data in this paper, along with previous reports (Zhao et al., 2005b; Wang et al., 2004), suggest that transport of pemetrexed, a new-generation antifolate now in clinical use, would be especially favored in solid tumors because of its high affinity for PCFT/HCP1 at acidic and neutral pH.

Besides its role in cellular transport, the PCFT/HCP1 may contribute to folate receptor-mediated endocytosis (Anderson et al., 1992). In this process, folate binds to glycosyl-phosphoinositol (GPI)-linked folate receptors at the cell surface, which are internalized in endocytic vesicles. Within the cytoplasm, the vesicles acidify, resulting in a marked transvesicular proton gradient. Acidification results in the dissociation of folate from the receptor and a strong driving force that would favor folate export from the vesicle via the PCFT/HCP1 (Murphy et al., 1984; Paulos et al., 2004). Similarly, PAT1-mediated export of amino acids from lysosomal vesicles in brain neurons has been proposed in addition to the role of this proton-coupled transporter in intestinal amino acid absorption (Boll et al., 2002; Sagne et al., 2001).

The identification of a molecular basis underlying folate transport mediated by a proton-coupled carrier offers a new dimension to the understanding of the physiology of folate transport, in particular, intestinal folate absorption and the mechanism of delivery of folates to peripheral tissues in which this activity is expressed. The molecular basis for hereditary folate malabsorption has been established. It is now possible to assess the role that alterations in this transporter might play in folate deficiency conditions. The observation that patients with this disease have no evidence of neural tube defects and that neurological deficits and other signs and symptoms appear months after birth implies that this gene is not absolutely required for delivery of folates to cells in the neural crest during embryonic neural tube formation. Rather, polymorphisms or mutations in this gene might contribute to *maternal* folate deficiency, especially in the developing world, compounding dietary folate deficiency and thereby increasing the chances of neural tube defects in the devel-

oping embryo (Eichholzer et al., 2006). Indeed, the incidence of hereditary folate malabsorption may be greater than previously appreciated, since most infants with this disorder in areas with endemic folate deficiency would be expected to die early in infancy, undiagnosed.

EXPERIMENTAL PROCEDURES

Cell Lines and Cell Culture Conditions

HeLa, HepG2, and Caco2 cells were obtained from the American Type Tissue Collection (Manassas, Va). HeLa, HeLa-R5, and HepG2 cells were maintained in RPMI 1640 medium. HeLa-R1 cells were maintained in the same medium at pH 6.9 in the presence of 500 nM MTX. Caco2 cells were grown in DMEM. All media were supplemented with 10% fetal bovine serum (Gemini Bio-Products, Calabasas, CA), 2 mM glutamine, 20 μ M 2-mercaptoethanol, 100 units/ml penicillin, and 100 μ g/ml streptomycin.

Reagents

[3 H]folic acid, [3 H]MTX, [3 H](6S)5-FTHF, and [3 H](6S)5-MTHF were obtained from Moravak Biochemicals (Brea, CA) and purity monitored and maintained by HPLC. (6S)5- and (6R)5-FTHF and (6S)5-MTHF were obtained from Schircks Laboratories (Jona, Switzerland). PT523, an antifolate analog, was a gift from Andre Rosowsky (Dana-Farber Cancer Institute, Boston, MA). Folic acid, MTX, FCCP, hemin, estrone-3-sulfate, taurocholic acid, cholic acid, sulfobromophthalein, and para-amino hippurate were obtained from Sigma-Aldrich (St. Louis, MO). Hemin was dissolved in DMSO as a 5 mM stock solution. FCCP was dissolved in 95% ethanol to a concentration of 5 mM.

Database Mining of the Human Genome

The Ensembl human peptide database was blasted with the search parameter of Distant Homology to identify distant homologues using the conserved domains across species of the three SLC19 family members (GenBank accession number pfam01770.12) and the human reduced folate carrier (GenBank accession number NP_919231) as query. The predicted proteins, with similarity to SLC19 family transporters and unknown function, were chosen and used for subsequent screening of differential mRNA expression between HeLa-R5 and HeLa-R1 cells by RT-PCR.

Cloning and Construction of G21

The open reading frame of G21 was amplified from cDNA of HeLa-R5 cells with *pfuUltra* DNA polymerase (Stratagene, Cedar Creek, TX) and primers that contain BglII restriction sites (underlined in Table S1) and subsequently cloned into the BglII site of the pSPT64 vector for synthesis of capped sense G21 cRNA from the SP6 promoter using the mMESSAGING MACHINES system (Ambion, Austin, TX), and into the BamHI site of pcDNA3.1(+) to generate pcDNA3.1(+)-G21.

Construction of G21 shRNA

The *Silencer* Express (Human U6) kit (Ambion, Austin, TX) was used according to the manufacturer's protocol to produce shRNA expression cassettes (SECs), which were screened by transient transfection into HeLa cells followed by measurement of MTX initial uptake and quantitative RT-PCR of G21 mRNA. The most effective SEC targeting G21 mRNA (1000-ACTAATCGGCTATGGTTCT-1020; GenBank accession number NM_080669) and the negative SEC were cloned into the pSEC hygromycin vector (Ambion). A commercial shRNA targeting G21 mRNA (841-CGATCCATTGTCCAGCTCTAT-861) and a negative nonsilencing shRNA in a pSM2 retroviral vector were obtained from Open Biosystems (Huntsville, AL).

Transfection

Transfection of plasmid DNA was performed in HepG2, HeLa, and Caco2 cells with Lipofectamine 2000 (Invitrogen). HepG2 cells, stably

transfected with either pcDNA3.1(+) or pcDNA3.1(+)-G21, were generated by G418 selection (600 $\mu\text{g}/\text{ml}$). Double selection with puromycin (5 $\mu\text{g}/\text{ml}$) and hygromycin (50 $\mu\text{g}/\text{ml}$) was adopted to obtain stably transfected Caco2 cells with both G21-silencing shRNA vectors, or with both nonsilencing negative control plasmids.

Amaxa Nucleofection of G21 siRNA Oligonucleotides

The Nucleofector II unit and the Nucleofector cell line kit T (Amaxa Inc., Gaithersburg, MD) were employed to nucleofect Caco2 cells with SMARTpool siRNA containing four different siRNA duplexes (catalog #L-018653, Dharmacon, Inc., Lafayette, CO) that target G21 mRNA or siCONTROL nontargeting siRNAs (catalog #D-001210-01, Dharmacon), which lack homology to any human gene. The nucleofected cells were assayed on day 3 postseeding for initial [^3H]MTX uptake and G21 mRNA expression by quantitative RT-PCR.

Uptake Studies in *Xenopus* Oocytes

Defolliculated *Xenopus laevis* oocytes were prepared as described (Jansen and Akabas, 2006) and injected with 50 nl of water or G21 cRNA (30 ng). Radiotracer uptake was determined 3 or 4 days later. Seven to ten oocytes were incubated in 500 μl of modified Barth's solution [MBS; 88 mM NaCl, 2.4 mM NaHCO_3 , 2.5 mM Na pyruvate, 1 mM KCl, 0.82 mM MgSO_4 , 0.41 mM CaCl_2 , 0.3 mM $\text{Ca}(\text{NO}_3)_2$, 15 mM MES or HEPES], and uptake of tritiated folate substrates was assessed at room temperature. Uptake was halted by the addition of ice-cold MBS (pH 7.5). Oocytes were washed ten times thereafter and solubilized with 10% SDS for measurement of radioactivity. To collapse the pH gradient across the oocyte membrane, seven to ten oocytes were incubated in MBS (pH 5.5) containing 0, 10, 20, 40, or 60 μM FCCP for 20 min, and uptake of transport substrates was assessed at pH 5.5.

Transport of Folates in HepG2, HeLa, and Caco2 Cells

Initial uptake of tritiated folates in HepG2, HeLa, or Caco2 cells was assessed using a protocol designed for rapid uptake determinations in cells growing in monolayer culture in liquid scintillation vials (Sharif and Goldman, 2000), except that cells were incubated at pH 7.4 and 37°C for 20 min before initiation of uptake. Substrate uptake was normalized to protein content.

Electrophysiological Analyses in *Xenopus* Oocytes

Defolliculated oocytes were injected with 50 nl of water (control) or G21 cRNA (50 ng), and kept at 17°C in horse serum medium (82.5 mM NaCl, 2.5 mM KCl, 1 mM MgCl_2 , 2.3 mM CaCl_2 , 5 mM HEPES, 5% horse serum [pH 7.5]). Electrophysiological recordings were conducted 3–7 days after cRNA injection in buffer (90 mM NaCl, 1 mM KCl, 1 mM MgCl_2 , 1.8 mM CaCl_2 , 5 mM TRIS, 5 mM MES) as described previously (Jansen and Akabas, 2006). Oocyte holding potential was -80 mV for K_m determination. For current-voltage (I-V) relationships, from a -60 mV holding potential step changes in membrane potential were applied for 2 s in 10 mV increments between -100 and 30 mV in the absence and presence of substrate.

Production of Peptide Antibody and Immunofluorescence

To generate antisera to human G21 protein, a peptide ([C]ADPH LEFQQFPQSP) corresponding to amino acids 446–459 of this protein was synthesized, conjugated with KLH, and injected into rabbits by Open Biosystems. The IgG fraction was isolated from the antiserum using a protein A-conjugated agarose column (Bio-Rad, Hercules, CA), and antibodies specific for G21 were purified with the Sulfolink Trial Kit (Pierce, Rockford, IL). Immunofluorescence was performed using affinity-purified anti-G21 and FITC-conjugated swine anti-rabbit antibody (Dako, Carpinteria, CA). HeLa cells were permeabilized with 0.2% Triton X-100 in phosphate buffer (PBS) at pH 7.4 for 15 min. The stained samples were mounted on slides with Vectashield mounting medium containing 1.5 $\mu\text{g}/\text{ml}$ propidium iodide (Vecta Laboratories, Burlingame, CA).

SDS-PAGE and Western Blotting

Water- and G21 cRNA-injected oocytes were homogenized in MBS with a protease inhibitor cocktail (Sigma-Aldrich). The homogenate was spun at 1000 \times g and 4°C for 5 min to collect supernatant, and the membrane fraction was pelleted by centrifugation at 13,200 \times g and 4°C for 30 min and resuspended in MBS with protease inhibitors. To obtain HepG2 cell membranes, cells were incubated on ice for 30 min in hypotonic buffer (50 mM Na_2HPO_4 , 1 mM EDTA [pH 7.4]) containing protease inhibitors, following which the membrane fraction was pelleted by centrifugation at 13,200 \times g and 4°C for 10 min and resuspended in the same buffer. SDS-PAGE and protein blotting were conducted to detect G21 protein using rabbit anti-G21 antibody and secondary goat anti-rabbit IgG-horseradish peroxidase conjugate (Cell Signaling Technology, Danvers, MA).

Northern Blotting

A human PolyA⁺ northern RNA blot containing polyA⁺ RNA (2 μg per lane) of 12 tissues (Origene, Rockville, MD) was hybridized with ^{32}P -dCTP-labeled cDNA probes from a G21 cDNA segment (97–396 bp; GenBank accession number NM_080669) overnight at 42°C followed by four 20 min high-stringency washes at 65°C. β -actin mRNA was probed as the loading control.

Quantitative RT-PCR

cDNA was synthesized from DNase I-treated total RNA from HeLa, HeLa-R5, HeLa-R1, and Caco2 cells with Superscript Reverse Transcriptase II (Invitrogen). cDNAs of the human digestive system were obtained from Clontech (Mountain View, CA). Real-time PCR was performed with SYBR green PCR Master Mix (Applied Biosystems, Foster City, CA) and primers specific for G21 (Table S1). G3PDH or β -actin was simultaneously amplified with specific primers (Table S1) as housekeeping genes to normalize the G21 expression.

Analysis of G21 in a Family with Hereditary Folate Malabsorption

Members of a family with hereditary folate malabsorption were studied according to a protocol approved by the Albert Einstein College of Medicine IRB (CCI #2006-279), and informed consent in the subjects' native language was obtained. Whole blood was used for isolation of genomic DNA by a Genomic DNA Purification Kit (Gentra Systems, Minneapolis, MN) and to generate EBV-transformed human B-lymphoblastoid cell lines in the Einstein Human Genetics Cell Culture Core. Each G21 exon with flanking regions was amplified using *Taq* DNA polymerase, Q-solution (Qiagen, Valencia, CA), and primers listed in Table S2. G21 or RFC cDNA was amplified from lymphoblastoid cells by RT-PCR. PCR products were gel purified and sequenced in an ABI 3730 DNA Analyzer (Applied Biosystems). The mutated region was verified by sequencing both DNA strands. An expression vector of the mutated G21 in which exon 3 was skipped (GenBank accession number BC010691) was purchased from Open Biosystems and, along with pcDNA3.1(+)-G21 (wild-type), was used for an assay of transport function. Western blot analysis on whole-cell lysate and cellular localization were performed as described above.

Supplemental Data

The Supplemental Data include one supplemental figure and two supplemental tables and can be found with this article online at <http://www.cell.com/cgi/content/full/127/5/917/DC1>.

ACKNOWLEDGMENTS

This work was supported by grants CA82621 (I.D.G.) and GM77660 (M.H.A.) from the National Institutes of Health. We thank Dr. Alan Finkelstein for helpful discussions.

Received: August 18, 2006
 Revised: September 19, 2006
 Accepted: September 27, 2006
 Published: November 30, 2006

REFERENCES

- Anderson, R.G.W., Kamen, B.A., Rothberg, K.G., and Lacey, S.W. (1992). Potocytosis: Sequestration and transport of small molecules by caveolae. *Science* 255, 410–411.
- Benz, R., and McLaughlin, S. (1983). The molecular mechanism of action of the proton ionophore FCCP (carbonylcyanide p-trifluoromethoxyphenylhydrazine). *Biophys. J.* 41, 381–398.
- Boll, M., Foltz, M., Rubio-Aliaga, I., Kottra, G., and Daniel, H. (2002). Functional characterization of two novel mammalian electrogenic proton-dependent amino acid cotransporters. *J. Biol. Chem.* 277, 22966–22973.
- Eichholzer, M., Tonz, O., and Zimmermann, R. (2006). Folic acid: A public-health challenge. *Lancet* 367, 1352–1361.
- Geller, J., Kronn, D., Jayabose, S., and Sandoval, C. (2002). Hereditary folate malabsorption: Family report and review of the literature. *Medicine (Baltimore)* 81, 51–68.
- Hagenbuch, B., and Meier, P.J. (2003). The superfamily of organic anion transporting polypeptides. *Biochim. Biophys. Acta* 1609, 1–18.
- Helmlinger, G., Yuan, F., Dellian, M., and Jain, R.K. (1997). Interstitial pH and pO₂ gradients in solid tumors in vivo: High-resolution measurements reveal a lack of correlation. *Nat. Med.* 3, 177–182.
- Hidalgo, I.J., Raub, T.J., and Borchardt, R.T. (1989). Characterization of the human colon carcinoma cell line (Caco-2) as a model system for intestinal epithelial permeability. *Gastroenterology* 96, 736–749.
- Horne, D.W. (1993). Transport of folates and antifolates in liver. *Proc. Soc. Exp. Biol. Med.* 202, 385–391.
- Jansen, M., and Akabas, M.H. (2006). State-dependent cross-linking of the M2 and M3 segments: Functional basis for the alignment of GABAA and acetylcholine receptor M3 segments. *J. Neurosci.* 26, 4492–4499.
- Koepsell, H., and Endou, H. (2004). The SLC22 drug transporter family. *Pflugers Arch.* 447, 666–676.
- Mason, J.B., and Rosenberg, I.H. (1994). Intestinal absorption of folate. In *Physiology of the Gastrointestinal Tract*, L.R. Johnson, ed. (New York: Raven Press), pp. 1979–1995.
- Mason, J.B., Shoda, R., Haskell, M., Selhub, J., and Rosenberg, I.H. (1990). Carrier affinity as a mechanism for the pH-dependence of folate transport in the small intestine. *Biochim. Biophys. Acta* 1024, 331–335.
- Matherly, L.H., and Goldman, D.I. (2003). Membrane transport of folates. *Vitam. Horm.* 66, 403–456.
- McEwan, G.T., Lucas, M.L., Denvir, M., Raj, M., McColl, K.E., Russell, R.I., and Mathan, V.I. (1990). A combined TDDA-PVC pH and reference electrode for use in the upper small intestine. *J. Med. Eng. Technol.* 14, 16–20.
- Murphy, R.F., Powers, S., and Cantor, C.R. (1984). Endosome pH measured in single cells by dual fluorescence flow cytometry: Rapid acidification of insulin to pH 6. *J. Cell Biol.* 98, 1757–1762.
- Opladen, T., Ramaekers, V.T., Heimann, G., and Blau, N. (2006). Analysis of 5-methyltetrahydrofolate in serum of healthy children. *Mol. Genet. Metab.* 87, 61–65.
- Paulos, C.M., Reddy, J.A., Leamon, C.P., Turk, M.J., and Low, P.S. (2004). Ligand binding and kinetics of folate receptor recycling in vivo: Impact on receptor-mediated drug delivery. *Mol. Pharmacol.* 66, 1406–1414.
- Sagne, C., Agulhon, C., Ravassard, P., Darmon, M., Hamon, M., El Mestikawy, S., Gasnier, B., and Giros, B. (2001). Identification and characterization of a lysosomal transporter for small neutral amino acids. *Proc. Natl. Acad. Sci. USA* 98, 7206–7211.
- Said, H.M. (2004). Recent advances in carrier-mediated intestinal absorption of water-soluble vitamins. *Annu. Rev. Physiol.* 66, 419–446.
- Selhub, J., and Rosenberg, I.H. (1981). Folate transport in isolated brush border membrane vesicles from rat intestine. *J. Biol. Chem.* 256, 4489–4493.
- Sharif, K.A., and Goldman, I.D. (2000). Rapid determination of membrane transport parameters in adherent cells. *Biotechniques* 28, 926–928.
- Shayeghi, M., Latunde-Dada, G.O., Oakhill, J.S., Laftah, A.H., Takeuchi, K., Halliday, N., Khan, Y., Warley, A., McCann, F.E., Hider, R.C., et al. (2005). Identification of an intestinal heme transporter. *Cell* 122, 789–801.
- Stover, P.J. (2004). Physiology of folate and vitamin B12 in health and disease. *Nutr. Rev.* 62, S3–S12.
- Wang, Y., Zhao, R., and Goldman, I.D. (2004). Characterization of a folate transporter in HeLa cells with a low pH optimum and high affinity for pemetrexed distinct from the reduced folate carrier. *Clin. Cancer Res.* 10, 6256–6264.
- Wang, Y., Rajgopal, A., Goldman, I.D., and Zhao, R. (2005). Preservation of folate transport activity with a low-pH optimum in rat IEC-6 intestinal epithelial cell lines that lack reduced folate carrier function. *Am. J. Physiol. Cell Physiol.* 288, C65–C71.
- Wike-Hooley, J.L., Haveman, J., and Reinhold, H.S. (1984). The relevance of tumour pH to the treatment of malignant disease. *Radiother. Oncol.* 2, 343–366.
- Zhao, R., Gao, F., Hanscom, M., and Goldman, I.D. (2004). A prominent low-pH methotrexate transport activity in human solid tumor cells: Contribution to the preservation of methotrexate pharmacological activity in HeLa cells lacking the reduced folate carrier. *Clin. Cancer Res.* 10, 718–727.
- Zhao, R., Chattopadhyay, S., Hanscom, M., and Goldman, I.D. (2005a). Antifolate resistance in a HeLa cell line associated with impaired transport independent of the reduced folate carrier. *Clin. Cancer Res.* 10, 8735–8742.
- Zhao, R., Hanscom, M., and Goldman, I.D. (2005b). The relationship between folate transport activity at low pH and reduced folate carrier function in human Huh7 hepatoma cells. *Biochim. Biophys. Acta* 1715, 57–64.